*Malaysian Journal of Analytical Sciences, Vol 22 No 6 (2018): 921 - 930*
*DOI: https://doi.org/10.17576/mjas-2018-2206-01*

**MALAYSIAN JOURNAL OF ANALYTICAL SCIENCES**
***Published by The Malaysian Analytical Sciences Society***
**ISSN 1394 - 2506**

# THE PHYSICAL AND ELECTROCHEMICAL CHARACTERISTIC OF GOLD NANOPARTICLES SUPPORTED PEDOT/GRAPHENE COMPOSITE AS POTENTIAL CATHODE MATERIAL IN FUEL CELLS

## (Pencirian Fizikal dan Elektrokimia Komposit Zarah Nano Aurum Disokong PEDOT/Grafin sebagai Bahan Katod Berpotensi dalam Sel Bahan Api)

Nurul'ain Basyirah Muhamad and Farhanini Yusoff*

*School of Marine and Environmental Sciences,*
*Universiti Malaysia Terengganu, 21030 Kuala Nerus, Terengganu, Malaysia*

**Corresponding author: farhanini@umt.edu.my*

Received: 2 August 2018; Accepted: 13 November 2018

**Abstract**

Gold nanoparticles/poly(3,4-ethylenedioxythiophene)/reduced graphene oxide (denoted as AuNPs/PEDOT/rGO) was synthesized as an electrocatalyst of cathode materials for used in fuel cells. The AuNPs/PEDOT/rGO catalyst was prepared by chemical deposition of AuNPs/PEDOT onto rGO sheets. The physical properties of composite were characterized by X-ray diffraction (XRD), scanning electron microscopy (SEM), Brunauer-Emmett-Teller (BET) and thermogravimetric analysis (TGA). The SEM results confirm the AuNPs is successfully attached on PEDOT/rGO sheets, while the XRD pattern confirmed the existence of crystallographic structure of composite. Analysis of thermogravimetry revealed the decomposition of synthesized composite is below 100 °C, where it is suitable for cathode material in fuel cells. For the fabrication of modified electrode, 10 µL of composite suspension was drop-casted on glassy carbon electrode (GCE) surface. Meanwhile, cyclic voltammetry and electrochemical impedance spectroscopy were used to study the electrochemical behaviour of modified electrode in in 1.0 M KCl solution with a reference to 5.0 mM $K_4[Fe(CN)_6]$ redox system. The result demonstrates that AuNPs/PEDOT/rGO catalyst enhance the high conductivity and charge transfer where it is useful as a material for cathode catalyst in fuel cells.

**Keywords**: gold nanoparticles, poly(3,4-ethylenedioxythiophene), reduced graphene oxide, cathode catalyst, fuel cells

**Abstrak**

Zarah nano aurum/poli(3,4-etilenadioxitiopena)/grafin oksida terturun (dilabel sebagai AuNPs/PEDOT/rGO) telah disintesis sebagai elektropemangkin bahan katod untuk digunakan dalam sel bahan api. Pemangkin AuNPs/PEDOT/rGO telah disediakan melalui pemendapan kimia AuNPs/PEDOT ke dalam lembaran rGO. Sifat fizikal komposit telah dicirikan oleh pembelauan sinar-X (XRD), mikroskop imbasan elektron (SEM), Brunauer-Emmett-Teller (BET) dan analisis termogravimetrik (TGA). Hasil SEM telah mengesahkan AuNPs telah berjaya melekat di lembaran PEDOT/rGO, sementara corak XRD mengesahkan kehadiran struktur kristalografi komposit. Analisis termogravimetrik telah membuktikan penguraian komposit yang telah disintesis di bawah 100 °C dimana ia sesuai digunakan sebagai bahan katod untuk sel bahan api. Untuk fabrikasi elektrod diubahsuai, setiap 10µL pemendapan komposit telah dititik alas pada permukaan elektrod karbon berkaca (GCE). Sementara itu, voltametri berkitar dan spektroskopi elektrokimia impedans telah digunakan untuk mengkaji sifat elektrokimia elektrod diubahsuai di dalam cecair 1.0 M KCl merujuk kepada sistem redoks 5.0 mM $K_4[Fe(CN)_6]$. Keputusan menunjukkan pemangkin AuNPs/PEDOT/rGO/GCE meningkatkan konduktiviti yang tinggi dan pemindahan cas dimana ia berguna sebagai bahan untuk pemangkin katod dalam sel bahan api.

**Kata kunci:** zarah nano aurum, poli(3,4-etilenadioxitiopena), grafin oksida terturun, pemangkin katod, sel bahan api

## Introduction

As the world moves towards renewable and sustainable energy, fuel cells (FCs) technology gained attention as a source to replace a combustion engine in vehicles. The good performance of FCs such as high reliability, quite operation and low maintenance capability making it has a capability used in wide application such as power generation, power transportation and portable power generation. In spite of FCs has an attraction as a green technology, the development of FCs still low due to the high cost and lack of suitable materials, especially for cathode electrode [1]. At the current stage technology of FCs, the Platinum (Pt) based electrode is used as a main cathode catalyst in FCs, however, the cost of Pt catalyst is extremely expensive and it is not stable yet [2].

Recent researches have been active in development of novel low cost electrocatalyst to replace high cost of commercial Pt-based electrode [3-5]. In order to replace Pt-based catalyst, gold nanoparticle (AuNPs) is promising a good metal catalyst compared to other metallic catalyst. The characteristic of AuNPs such as high stability and good resistant for oxidation making it is suitable as greener catalyst material. Additionally, the fabrication of AuNPs with others material can be considered for electrochemical applications, which is high catalytic activity of AuNPs in many reaction such as CO oxidation, methanol oxidation and redox reaction of oxygen [6].

Metal nanoparticles (NPs) decorated graphene sheets gained attracted in order to improve efficiency and stability of electrode materials. Up to date, numerous studies have been focused on the hybridization of graphene with AuNPs in electrochemical application [7-11]. Recent work has been reported that graphene sheets has an ability to decrease Pt particle size and existence a binding sites that provide strong interaction between Pt particles and graphene sheets [12]. Furthermore, the 2-dimensional carbon structure of graphene oxide (GO) with electrical and mechanical properties can be used effectively as electrocatalytic support materials. Meanwhile, reduced graphene oxide (rGO) with less oxygen functional group provide an active binding site for NPs and minimizing poisoning of electrocatalyst [13].

Indeed, conducting polymer/NPs hybrids has an ability as a novel composite materials with a synergetic and behaviour [14]. In addition, conjugated polymer with high conductivity such as poly(3,4-ethylenedioxythiophene) (PEDOT) as a substrate for deposition of NPs on graphene has a possibilities to achieve uniform dispersion and enhance a stability of NPs. The unique properties of PEDOT such as high electrochemical stability and catalytic activity making them excellent and high efficiency as a catalyst support [15]. PEDOT decorated graphene composite can be a good adhesion with NPs and improve the adsorption, catalytic and conductive properties leading for good performance for cathode catalyst materials.

Herein, the purpose of this work is to prepare AuNPs/PEDOT/rGO composite as a potential material for cathode electrode in FCs. For the comparison, rGO and PEDOT/rGO composite were also prepared by one-pot chemical method. For the physical and electrochemical characteristic, the composites were characterized *via* several instruments and electrochemical technique.

## Materials and Methods

### Chemicals and reagents

Graphite powder, chloroauric acid ($HAuCl_4$), sodium nitrate ($NaNO_3$), 3,4-ethylenedioxythiophene (EDOT) monomer and sodium borohydride ($NaBH_4$) were purchased form Sigma Aldrich, USA. Sulphuric acid ($H_2SO_4$, 95-98%), potassium permanganate ($KMnO_4$), hydrochloric acid (HCl, 5%), ethanol absolute, potassium chloride (KCl) and potassium ferrocyanide ($K_4[Fe(CN)_6]$) were supplied from Hamburg, German. Alumina powder supplied by Bendosen and was used for the clean of electrode's surface.

### Physical characterization

The surface morphology of catalyst was determined using scanning electron microscopy (SEM) JEOL JSM 6360LA at the operational voltage of 5 kV. X-ray diffraction (XRD) pattern was conducted using X-ray Diffractometer, Rigaku Miniflex II using CuKα line ($\lambda$ = 1.540598 Å) as radiation source. Brunauer-Emmett-Teller (BET) surface area analyzer with a heating rate of 10 ºC over a temperature range of 20ºC-800ºC in a nitrogen atmosphere was

performed by ASAP 2020 Micrometrics, USA.Thermogravimetric analyses (TGA) was carried out using Mettler Toledo thermal analysis system TGA/DSC 1 with a heating temperature over a range of 20 ºC – 800 ºC.

**Electrochemical characterization**

The electrocatalytic activity of modified electrode was determined using cyclic voltammetry (CV) technique performed by Potentiostat/Galvanostat Autolab PGSTAT302N controlled with NOVA 1.10 software. The cyclic voltammogram was scanned in the potential range of -0.2 V to 0.8 V at the 100 mV/s of scan rate. Glassy carbon electrode (GCE) with or without catalyst, platinum wire electrode and Ag/AgCl (3.0 M KCl) were served as working electrode, counter electrode and reference electrode, respectively. Electrochemical impedance spectroscopy (EIS) measurement was conducted using Autolab FRA32M with the frequency range of 1 Hz to 100,00 Hz and AC voltage 0.20 V.

**Preparation of GO**

GO was prepared according to modified Hummers method [16]. In a typical synthesis, 3 g of graphite powder and 1.5 g of $NaNO_3$ was poured into 23 ml of $H_2SO_4$ under rapid stirring. After 30 minutes, 4 g of $KMnO_4$ was slowly added into mixture solution. The solution was kept under 10 ºC. Next, the mixture solution was transferred into 35±5 ºC water bath and kept stirring for 30 minutes, then the mixture solution was diluted with 46 ml of deionized water and the temperature was raised up to 98 ºC. The mixture solution was diluted again with 140 ml of deionized water and left it stirred for 30 minutes. Finally, the mixture solution was treated with 10 ml of $H_2O_2$ to stop the reaction. Further, the mixture solution was washed with 5% of HCl and repeated centrifuging with deionized water. The synthesized product was dried in oven at 60 ºC.

**Preparation of AuNPs/PEDOT/rGO**

To synthesis AuNPs/PEDOT/rGO, 25 ml of EDOT in ethanol solution (22.5 mM) was poured into 350 ml of $HAuCl_4$ solution (0.65 mM) under a rapid stirring (750 rpm). The solution was immediately turned into dark blue solution. After 4 hours, 25 ml of GO suspension (0.5 mg/ml) was added into mixture solution, and then the AuNPs/PEDOT/GO was sonicated for 2 hours until homogenous. After that, 27.5 ml of $NaBH_4$ (0.16 M) was added drop by drop into mixture solution under rapid stirring. The reaction was continuously stirring for 6 hours. Finally, the AuNPs/PEDOT/rGO (Scheme 1) composite was obtained by washing a mixture solution using centrifugation with methanol and deionized water for several times, then dried it in an oven at 60 ºC. For comparison, rGO and PEDOT/rGO were prepared under a same condition.

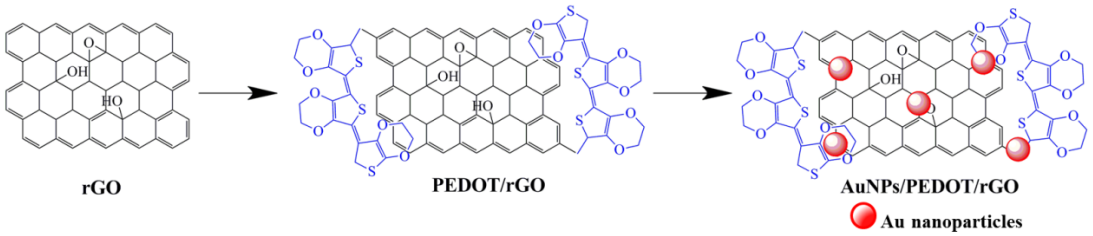


Scheme 1. Schematic diagram for the formation of AuNPs/PEDOT/rGO

**Electrode fabrication**

A bare GCE was pre-polished with alumina slurry and then rinsed with deionized water before and after use. For prepare catalyst suspension, 1 mg of each catalyst was dissolved in 1 ml of deionized water and was sonicated for 30 minutes. Then, 10 µL of each suspension is casted on the GCE surface and allowing excessive water to evaporate at room temperature. The modified electrode was carefully rinsed with deionized water before and after an electrochemical experiment.

## Results and Discussion

### Physical characterization

The SEM images were recorded to determine the morphology of graphene sheets before and after modified with AuNPs and PEDOT as presented in Figure 1. The 2-dimenisonal of rGO surface (Figure 1(a)) is wrinkle with fold structure and rGO layers are restacked together. This appearance is might be due to the interlocking between nanoscale and GO sheets, which have led to the increasing of surface area and decreasing of surface energy [17]. In Figure 1(b), the surface of rGO with modified PEDOT has produced more rough wrinkles due to the PEDOT embedded on the rGO sheets. It is also evident that PEDOT/rGO catalyst can provide a sufficient surface area for the attachment of AuNPs and enhance an electron transfer for modified electrode [18]. In addition, the morphology of AuNPs/PEDOT/rGO surface clearly shows AuNPs was agglomerated on PEDOT/rGO sheets. It is clear the wrinkle surface of PEDOT/rGO sheet providing attachment sites and increase dispersity of AuNPs [19].

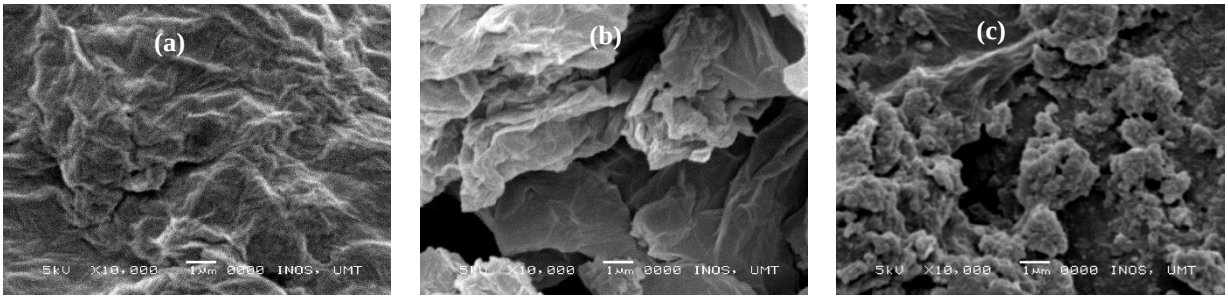


Figure 1. SEM results of (a) rGO; (b) PEDOT/rGO and (c) AuNPs/PEDOT/rGO at 10x magnification.

The XRD pattern of the phase structure for synthesized catalyst is depicted in Figure 2. The XRD pattern of GO in Figure 2(a) shows a sharp peak (001) at 2θ = 10.62º, suggesting the existing of oxygen functional group attached at edge of GO sheets [20]. After chemical reduction of GO, the (001) diffraction peak of GO is disappear and shifted to 2θ = 23.01º indicating the oxygen functional group successfully removed and restoration of C-C bonding in rGO (Figure 2(b)) [21]. Furthermore, the XRD pattern of PEDOT/rGO in Figure 2(c) exhibits a broad peak at 2θ = 28.04º attributed from polymeric amorphous of PEDOT [22]. XRD pattern of AuNPs/PEDOT/rGO in Figure 2 (d) shows a broad peak at 2θ = 25.0º belongs to C of PEDOT and rGO and five sharp peaks appearing at 2θ as 38.05º, 44.17º, 64.52º, 77.30º and 81.84º that correspond to the Au(111), Au(200), Au(220),Au (311) and Au(222), respectively. Therefore, it reveals that the Au has been successfully reduced and growth on PEDOT/rGO sheets.

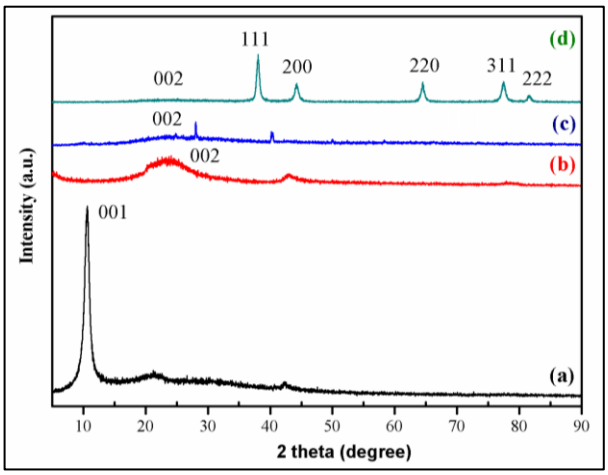


Figure 2. XRD results of (a) GO; (b) rGO; (c) PEDOT/rGO and (d) AuNPs/PEDOT/rGO.

From Table 1, the interlayer spacing ($\boldsymbol{d}$) is calculated using Bragg's formula (Eq. 1) [22]:

$$\boldsymbol{d}=\frac{\lambda}{2\sin\theta} \quad (1)$$

where $\boldsymbol{d}$ is interlayer spacing, λ is the wavelength of Cu Kα radiation (λ = 1.54 *Å*) and θ is the Bragg angle from highest value of FWHM (full width at half maximum), respectively. From the Eq.1, the value of GO (0.83 nm) is slightly higher due to the formation of oxygen group between graphene layer. The $\boldsymbol{d}$ value of rGO (0.39 nm) is much lower than GO signifying to the removal of oxygen group and restoration of conjugation of π-π interaction in rGO sheets [23]. The layer distance of PEDOT/rGO is 0.32 nm reflects to the closer packing of polymer matrix with graphene sheets [24], while the distance of AuNPs/PEDOT/rGO (0.21 nm) is much closer due to the AuNPs bind to PEDOT/rGO surface. The average of crystallite is obtained from Debye-Scherrer formula, and they were about GO (9.27 nm), rGO (0.97 nm), PEDOT/rGO (71.30 nm) and AuNPs/PEDOT/rGO (12.80 nm).

Table 1. Various parameter of catalyst obtained from XRD results

| **Composites** | ***2θ*** **(degree)** | **FWHM (degree)** | ***d*** **(nm)** | **D (nm)** |
|---|---|---|---|---|
| GO | 10.62 | 0.89 | 0.83 | 9.27 |
| rGO | 23.01 | 8.74 | 0.39 | 0.97 |
| PEDOT/rGO | 28.04 | 0.15 | 0.32 | 71.30 |
| AuNPs/PEDOT/rGO | 44.17 | 0.70 | 0.21 | 12.80 |

The surface area of synthesized composites was recorded using Brunauer-Emmett-Teller (BET) is listed in Table 2. The properties BET surface area of GO was measured is 400.58 $m^2g^{-1}$, which is far lower than theoretical value of graphene (~2620 $m^2g^{-1}$) which may be due to the incomplete oxidation of graphite and agglomeration of graphene sheet upon reduction [25]. However, the properties surface area of rGO is lower surface area compared to GO due to the removal of oxygen functional group which leading to rearrangement of spatial carbon atom. The deposition of PEDOT on rGO sheets resulted to the lowering BET surface area because of covering of polymeric structure of PEDOT on rGO sheets. Meanwhile, the specific surface area of AuNPs/PEDOT/rGO was increased twice than PEDOT/rGO corresponding to the incorporation of AuNPs has increased the surface area of composite.

Table 2. Surface area of GO, rGO, DOT/rGO and AuNPs/PEDOT/rGO

| **Composites** | **Properties BET surface area/ $m^2g^{-1}$** |
|---|---|
| GO | 400.58 |
| rGO | 211.27 |
| PEDOT/rGO | 8.18 |
| AuNPs/PEDOT/rGO | 21.07 |

Figure 3 shows TGA curves of rGO, PEDOT/rGO and AuNPs/PEDOT/rGO under argon atmosphere at rate 10 ºC/min. The thermogram of rGO shows a two decomposition steps; the first step located at 57 ºC with 3.29% weight loss due to the loss of adsorbed water. The second decomposition step at 518 ºC, where 17.13% catalyst was decomposed corresponding to the pyrolysis of a carbon material in rGO. There is small amount of weight loss by rGO because of it does not contain a large amount of oxygen group [20]. Meanwhile, PEDOT/rGO catalyst also shows two decomposition steps. The first decomposition step takes places at 75 ºC due to the decomposition of oxygen group contain in rGO, then the second mass loss in range 300 ºC – 600 ºC, corresponding to 44.87%

decomposition of PEDOT material [26]. The thermogram of AuNPs/PEDOT/rGO also has two decomposition steps, the first step weight loss at 96 ºC due to the loss of water molecule adsorbed catalyst during catalyst preparation. The second step located at 493 ºC attributed to decomposition of PEDOT. The residual mass loss is about 49.76 % corresponding to AuNPs that it is more stable [27]. Therefore, the result suggests that the synthesize catalyst start to decompose below 100 ºC, where it is stable for material in FCs.

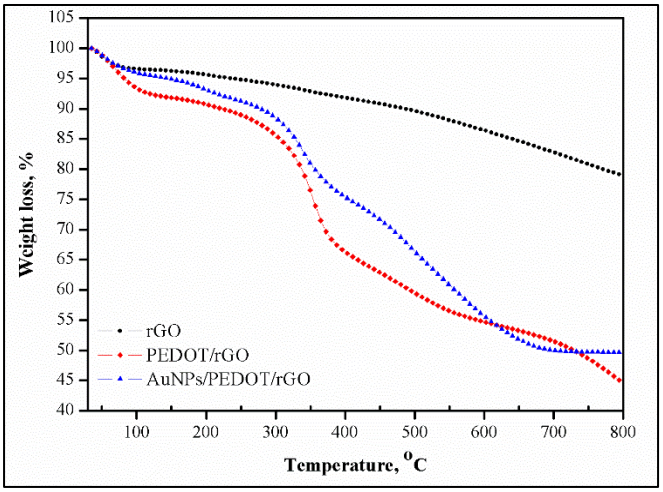


Figure 3. TGA curves of rGO, PEDOT/rGO and AuNPs/PEDOT/rGO

**Electrochemical behavior of modified electrode**

CV technique was performed to study the performance of modified electrode toward electrocatalytic activity. As shown in Figure 4(a), all the cyclic voltammogram of modified electrodes are well—defined peak quasi-reversible redox peak attributed to the stability of electron transfer between electrode surface and electrolyte. Specifically, rGO/GCE and PEDOT/rGO/GCE have a higher redox peak current and smaller peak separation compared to bare GCE. The increasing of the peak current is likely due to the electrical conductivity and electroactive surface area of rGO and PEDOT. However, the cyclic voltammogram of AuNPs/PEDOT/rGO/GCE shows the largest redox peak current, which probably due to the AuNPs provide a reaction sites for enhance larger effective surface area to facilitate transfer of $[Fe(CN)]^{-3/-4}$ electron [28].

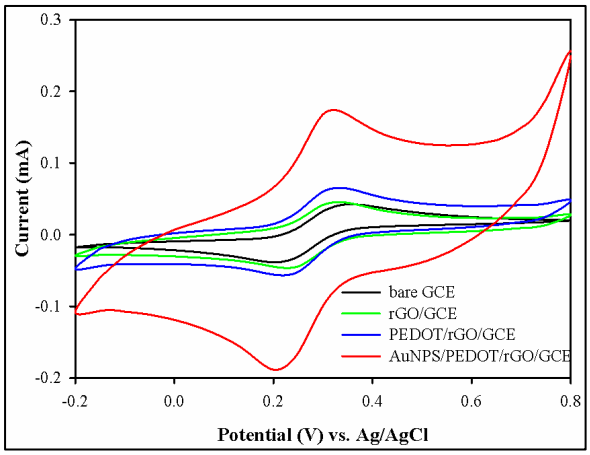


Figure 4. Cyclic voltammogram of bare GCE, rGO/GCE, PEDOT/rGO and AuNPs/PEDOT/rGO in 5.0 mM $K_4[Fe(CN)_6]$ of 1.0 M KCl solution at a scan rate of 100 mV/s

The effect of potential scan rate was studied on the AuNPs/PEDOT/rGO/GCE (Figure 5(a)). From the graph, the anodic and cathodic peaks are shifted to higher and lower current with the increasing of scan rate, respectively. This result revealed the AuNPs/PEDOT/rGO modified electrode has a fast electron transfer on the surface electrode indicating it has a good diffusion process and good rate capability [29]. In addition, the cyclic voltammogram of redox peaks show a similar shape for all scan rates means that the modified electrode is reversible. The specific capacitances (C) on the scan rate of modified electrodes were calculated by using Eq. 2 [30]:

$$C = \frac{I}{2.V.S.m} \tag{2}$$

where C is the specific capacitance (F/g), *I* is the integrated area of cyclic voltammogram (V A), S is the scan rate (V/s) and m is the mass (g) of composite. Figure 5(b) shows the dependence of capacitance of scan rate for all modified electrode. As can be seen, the trend of specific capacitance for all modified electrode is decrease with the increasing of scan rate where the highest specific capacitance is obtained at slower scan rate may be due to the better ion penetration on the surface of modified electrode. The highest potential window of AuNPs/PEDOT/rGO/GCE gives the largest capacitive value compared to others indicating the hybridization of AuNPs with PEDOT/rGO has a better contact between modified electrode and electrolyte.

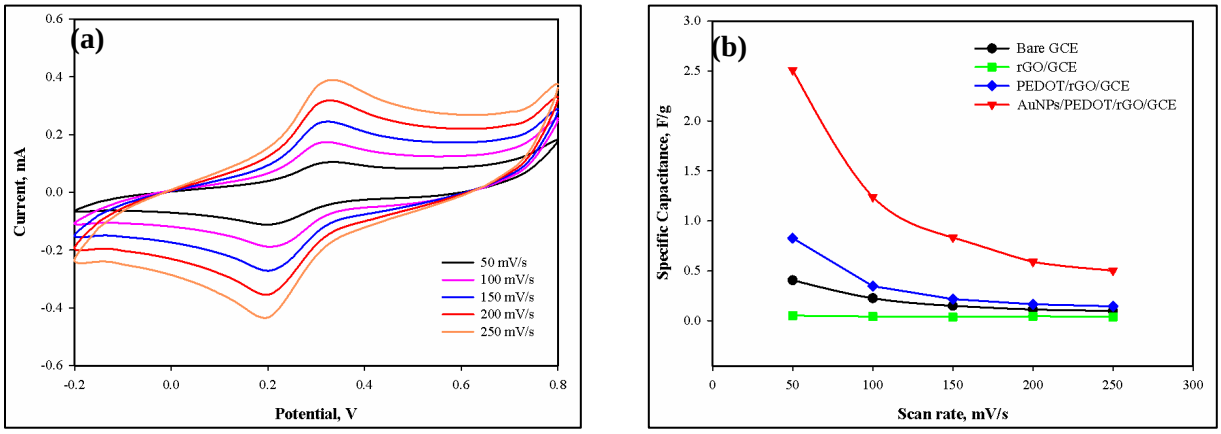


Figure 5. (a) Effect of scan rate on AuNPs/PEDOT/rGO/GCE and (b) plot of specific capacitance vs. scan rate of modified electrode. (Electrolyte solution: 5.0 mM $K_4[Fe(CN)_6]$ in 1.0 M KCl)

The charge-transfer resistance ($R_{ct}$) and double layer capacitance ($C_{dl}$) characteristic of modified electrode were conducted by EIS. The Nyquist plot typically presents a semicircle of $R_{ct}$ occur at electrode surface at high frequency and the linearly part of diffusion-controlled process ($Z_w$) at low frequency. In Figure 6(a), the $R_{ct}$ is only exhibit in bare GCE, but as the catalyst was casted on bare GCE, the $R_{ct}$ is decreased. This could be attributed to the positive charge from catalyst has an ability to attract a negative charge of $[Fe(CN)]^{-3/-4}$ ion and enhance electron transfer on electrode surface [31]. However, AuNPs/PEDOT/rGO/GCE exhibits the characteristic of kinetic and diffusion process at low frequencies indicating high conductive and capacitive behaviour due to the AuNPs as a modifier.

Figure 6(b) shows an elements proposed in modified Randles circuit were extracted from Nyquist plot. To obtained best fitting for Nyquist Plot, the R[C(RW)] Randles circuit for bare GCE is changed to R[(RW)C]Q for modified electrode. It can be seen from Table 3, the solution resistance ($R_s$) is decrease with the addition of catalyst on bare GCE. Meanwhile, the modified electrodes exhibit double capacitance processes, where the value of *n* is near to ideal capacitor. The apparent electron transfer rate constant ($K_{app}$) for modified electrodes were obtained from Eq. 3;

$$K_{app} = RT/F^2R_{ct}C \tag{3}$$

where R is the gas constant, T is temperature of system, F is Faraday constant, C is concentration of $[Fe(CN)]^{-3/-4}$. The value of $K_{app}$ is higher as the $R_{ct}$ is lower for AuNPs/PEDOT/rGO/GCE reveals this electrode is fastest electron transfer process compared to others as supported from CV result [32].

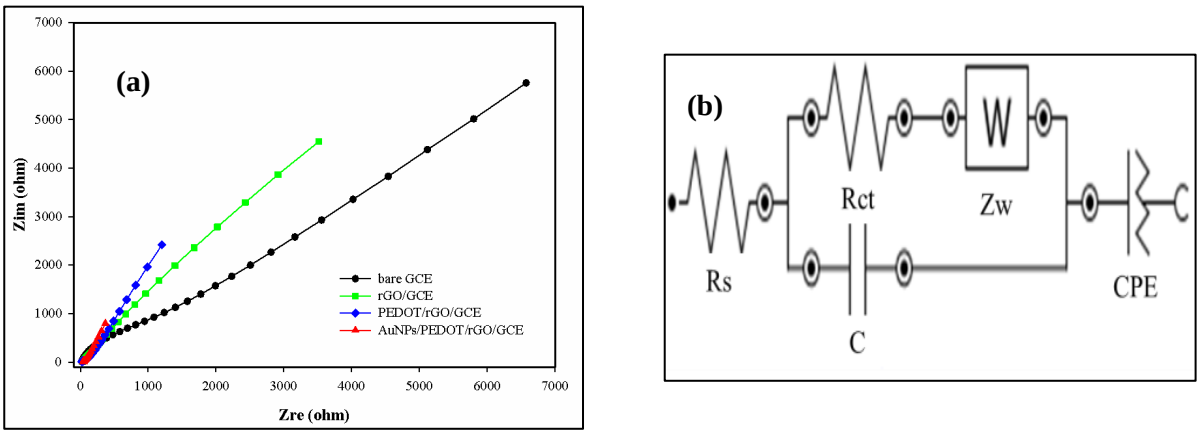


Figure 6. (a) Nyquist plot of modified electrode in 5.0 mM $K_4[Fe(CN)_6]$ and 1.0 M KCl solution and (b) Modified Randles equivalent circuit.

Table 3. Parameter's value of modified Randles equivalent circuit for all modified electrode

| **Modified Electrode** | **$R_s$ ($\Omega cm^2$)** | **$R_{ct}$ ($\Omega cm^2$)** | ***n*** | **$K_{app}$ ($cms^{-1}$)** |
|---|---|---|---|---|
| Bare GCE | 73.0 | 815 | 0.280 | $6.53 \times 10^{-5}$ |
| rGO/GCE | 61.0 | 63.8 | 0.788 | $8.34 \times 10^{-4}$ |
| PEDOT/rGO/GCE | 55.0 | 49.2 | 0.745 | $1.08 \times 10^{-3}$ |
| AuNPs/PEDOT/rGO/GCE | 43.7 | 6.85 | 0.832 | $7.77 \times 10^{-3}$ |

## Conclusion

In this work, AuNPs/PEDOT/rGO is successfully synthesized by facile chemical method as a new catalyst for cathode material in FCs. This study found that AuNPs as a modifier on PEDOT/rGO sheet has improved the performance of catalyst in terms of conductivity, capacity and charge transfer. The stability, thermal decomposition and sensitivity of AuNPs/PEDOT/rGO are recommended for a new catalyst in cathode materials of FCs. Future work would attempt to study the kinetic analysis and electrocatalytic activity of modified electrode on oxygen reduction reaction.

## Acknowledgements

The authors are grateful to Ministry of Education Research Acculturation Grant Scheme (RAGS) RAGS/1/20215/ST01/UMT/03/2 and Fundamental Research Grant Scheme (FRGS) FRGS/1/2017/STG01/ UMT/02/2 for financial support as well as Universiti Malaysia Terengganu for providing facilities for undertaking this research.

## References

1. Shao, M. (2015). Electrocatalysis in fuel cells. *Catalysts*, 5 (4): 2115-2121.
2. Holton, O. T. and Stevenson, J. W. (2013). The role of platinum in proton exchange membrane fuel cells. *Platinum Metals Review*, 57(4): 259-271.

3. Peera, S. G., Tintula, K. K., Sahu, A. K., Shanmugam, S., Sridhar, P. and Pitchumani, S. (2013). Catalytic activity of Pt anchored onto graphite nanofiber-poly (3, 4-ethylenedioxythiophene) composite toward oxygen reduction reaction in polymer electrolyte fuel cells. *Electrochimica Acta*, 108: 95-103.
4. Ferreira, P. J., Shao-Horn, Y., Morgan, D., Makharia, R., Kocha, S. and Gasteiger, H. A. (2005). Instability of Pt/C electrocatalysts in proton exchange membrane fuel cells a mechanistic investigation. *Journal of The Electrochemical Society*, 152(11): 2256-2271.
5. Zhang, L. and Xia, Z. (2011). Mechanisms of oxygen reduction reaction on nitrogen-doped graphene for fuel cells. *The Journal of Physical Chemistry C*, 115(22): 11170-11176.
6. Rad, A. G., Abbasi, H. and Afzali, M. H. (2011). Gold nanoparticles: Synthesizing, characterizing and reviewing novel application in recent years. *Physics Procedia*, 22: 203-208.
7. Choi, Y., Gu, M., Park, J., Song, H. K. and Kim, B. S. (2012). Graphene multilayer supported gold nanoparticles for efficient electrocatalysts toward methanol oxidation. *Advanced Energy Materials*, 2 (12): 1510-1518.
8. Hu, Y., Jin, J., Wu, P., Zhang, H. and Cai, C. (2010). Graphene–gold nanostructure composites fabricated by electrodeposition and their electrocatalytic activity toward the oxygen reduction and glucose oxidation. *Electrochimica Acta*, 56(1): 491-500.
9. Chen, J., Jia, C. and Wan, Z. (2014). Novel hybrid nanocomposite based on poly (3,4-ethylenedioxythiophene)/multiwalled carbon nanotubes/graphene as electrode material for supercapacitor. *Synthetic Metals*, 18: 69-76.
10. Shervedani, R. K. and Amini, A. (2014). Novel graphene-gold hybrid nanostructures constructed via sulfur modified graphene: preparation and characterization by surface and electrochemical techniques. *Electrochimica Acta*, 121: 376-385.
11. Ali, A., Zhang, Y., Jamal, R. and Abdiryim, T. (2017). Solid-state heating synthesis of poly(3,4-ethylenedioxythiophene)/gold/graphene composite and its application for amperometric determination of nitrite and iodate. *Nanoscale Research Letters*, 12(1): 568.
12. Fortunato, G. V., de Lima, F. and Maia, G. (2016). Oxygen-reduction reaction strongly electrocatalyzed by Pt electrodeposited onto graphene or graphene nanoribbons. *Journal of Power Sources*, 302: 247-258.
13. Dinesh, B. and Saraswathi, R. (2016). Enhanced performance of Pt and Pt–Ru supported PEDOT–RGO nanocomposite towards methanol oxidation. *International Journal of Hydrogen Energy*, 41(31): 13448-13458.
14. Rao, H., Chen, M., Ge, H., Lu, Z., Liu, X., Zou, P., Wang, X., He, H., Zeng, X. and Wang, Y. (2017). A novel electrochemical sensor based on Au@ PANI composites film modified glassy carbon electrode binding molecular imprinting technique for the determination of melamine. *Biosensors and Bioelectronics*, 87: 1029-1035.
15. Groenendaal, L., Zotti, G., Aubert, P. H., Waybright, S. M. and Reynolds, J. R. (2003). Electrochemistry of poly (3, 4-alkylenedioxythiophene) derivatives. *Advanced Materials*, 15(11): 855-879.
16. Hummers Jr, W. S. and Offeman, R. E. (1958). Preparation of graphitic oxide. *Journal of The American Chemical Society*, 80(6): 1339-1339.
17. Yang, J. and Gunasekaran, S. (2013). Electrochemically reduced graphene oxide sheets for use in high performance supercapacitors. *Carbon*, 51: 36-44.
18. Mao, X., Yang, W., He, X., Chen, Y., Zhao, Y., Zhou, Y., Yang, Y. and Xu, J. (2017). The preparation and characteristic of poly (3, 4-ethylenedioxythiophene)/reduced graphene oxide nanocomposite and its application for supercapacitor electrode. *Materials Science and Engineering: B*, 216: 16-22.
19. Liu, Z., Xu, J., Yue, R., Yang, T. and Gao, L. (2016). Facile one-pot synthesis of Au–PEDOT/rGO nanocomposite for highly sensitive detection of caffeic acid in red wine sample. *Electrochimica Acta*, 196: 1-12.
20. Park, S., An, J., Potts, J. R., Velamakanni, A., Murali, S. and Ruoff, R. S. (2011). Hydrazine-reduction of graphite-and graphene oxide. *Carbon*, 49(9): 3019-3023.
21. Zhang, X., Zhang, D., Chen, Y., Sun, X. and Ma, Y. (2012). Electrochemical reduction of graphene oxide films: preparation, characterization and their electrochemical properties. *Chinese Science Bulletin*, 57(23): 3045-3050.
22. Selvaganesh, S. V., Mathiyarasu, J., Phani, K. L. N. and Yegnaraman, V. (2007). Chemical synthesis of PEDOT–Au nanocomposite. *Nanoscale Research Letters*, 2(11): 546.

23. Saini, P., Sharma, R. and Chadha, N. (2017). Determination of defect density, crystallite size and number of graphene layers in graphene analogues using X-ray diffraction and raman spectroscopy. *Indian Journal of Pure & Applied Physics*, 55(9): 625-629.
24. Chen, L., Liu, W., Su, X., Xiao, S., Xie, H., Uher, C. and Tang, X. (2017). Chemical synthesis and enhanced electrical properties of bulk poly (3, 4-ethylenedioxythiophene)/reduced graphene oxide nanocomposites. *Synthetic Metals*, 229: 65-71.
25. Dreyer, D. R., Park, S., Bielawski. C. W. and Ruoff, R. S. (2010) The chemistry of graphene oxide. *Chemical Society Reviews*, 39: 228-240.
26. Li, Y. and Ni, X. (2016). One-step preparation of graphene oxide–poly(3,4-ethylenedioxythiophene) composite films for nonvolatile rewritable memory devices. *RSC Advances*, 6(20): 16340-16347.
27. Felix-Navarro, R. M., Beltran-Gastelum, M., Reynoso-Soto, E. A., Paraguay-Delgado, F., Alonso-Nuñez, G. and Flores-Hernandez, J. R. (2016). Bimetallic Pt–Au nanoparticles supported on multi-wall carbon nanotubes as electrocatalysts for oxygen reduction. *Renewable Energy*, 87: 31-41.
28. Yusoff, F., Mohamed, N., Aziz, A. and Ab Ghani, S. (2014). electrocatalytic reduction of oxygen at perovskite (BSCF)-MWCNT composite electrodes. *Materials Sciences and Applications*, 5(4): 199-211.
29. Azman, N. H. N., Lim, H. N. and Sulaiman, Y. (2016). Effect of electropolymerization potential on the preparation of PEDOT/graphene oxide hybrid material for supercapacitor application. *Electrochimica Acta*, 188: 785-792.
30. Dar, F. I., Moonoosawmy, K. R. and Es-Souni, M. (2013). Morphology and property control of Nio nanostructures for supercapacitor applications. *Nanoscale Research Letters*, 8(1): 363.
31. Zhang, Z., Zhu, H., Wang, X. and Yang, X. (2011). Sensitive electrochemical sensor for hydrogen peroxide using $Fe_3O_4$ magnetic nanoparticles as a mimic for peroxidase. *Microchimica Acta*, 174(1-2): 183-189.
32. Yusoff, F., Aziz, A., Mohamed, N. and Ab Ghani, S. (2013). Synthesis and characterizations of BSCF at different pH as future cathode materials for fuel cell. *International Journal of Electrochemical Science*, 8(8): 10672-10687.